Scientific Research Publishing

Open Journal of Fluid Dynamics, 2022, 12, 321-341
https://www.scirp.org/journal/ojfd
ISSN Online: 2165-3860
ISSN Print: 2165-3852

Soil Nature Effect Investigation on the Ground-to-Air Heat Exchanger for the Passive Cooling of Rooms

Kokou N'wuitcha[1], Yendouban Kolani[1], Yawovi Nougblega[1], Magolmèèna Banna[1], Belkacem Zeghmati[2]

[1]Department of Physics, Solar Energy Laboratory, University of Lome, Lome, Togo
[2]Department of Physics, Laboratory of Mathematics and Physics, University of Perpignan, Perpignan, France
Email: knwuitcha@gmail.com

How to cite this paper: N'wuitcha, K., Kolani, Y., Nougblega, Y., Banna, M. and Zeghmati, B. (2022) Soil Nature Effect Investigation on the Ground-to-Air Heat Exchanger for the Passive Cooling of Rooms. *Open Journal of Fluid Dynamics*, **12**, 321-341.
https://doi.org/10.4236/ojfd.2022.124016

Received: October 31, 2022
Accepted: December 23, 2022
Published: December 26, 2022

Abstract

The building sector consumes much energy either for cooling or heating and is associated to greenhouse gas emissions. To meet energy and environmental challenges, the use of ground-to-air heat exchangers for preheating and cooling buildings has recently received considerable attention. They provide substantial energy savings and contribute to the improvement of thermal comfort in buildings. For these systems, the ground temperature plays the main role. The present work aims to investigate numerically the influence of the nature of soil on the thermal behavior of the ground-to-air heat exchanger used for building passive cooling. We have taken into account in this work the influence of the soil nature by considering three types of dry soil: clay soil, sandy-clay soil and sandy soil. The mixed convection equations governing the heat transfers in the earth-to-air heat exchanger have been presented and discretized using the finite difference method with an Alternate Direction Implicit (ADI) scheme. The resulting algebraic equations are then solved using the algorithm of Thomas combined with an iterative Gauss-Seidel procedure. The results show that the flow is dominated by forced convection. The examination of the sensitivity of the model to the type of soil shows that the distributions of contours of streamlines, isotherms, isovalues of moisture are less affected by the variations of the nature of soil through the variation of the diffusivity of the soil. However, it is observed that the temperature values obtained for the clay soil are higher while the sandy soil shows lower temperature values. The values of the ground-to-air heat exchanger efficiency are only slightly influenced by the nature of the soil. Nevertheless, we note a slightly better efficiency for the sandy soil than for the sandy-clayey silt and clayey soils. This result shows that a sandy soil would be more suitable for geothermal system installations.

Keywords

Soil Temperature, Laminar Regime, Ground-To-Air Heat Exchanger, Heat Transfer, Geothermal System

1. Introduction

In recent years, there has been a rapid growth in global energy consumption due to population growth, increasing demand for services and comfort levels in buildings, as well as increasing dwell times in buildings. This high demand for energy leads to supply difficulties, depletion of fossil energy resources and severe environmental consequences such as ozone depletion, global warming and climate change.

The overall contribution of buildings to energy consumption, both residential and commercial, has been increasing steadily, reaching figures between 20 and 40% in developed countries, and has overtaken the other major sectors: industry and transport [1]. To reduce the energy consumption of buildings, several solutions exist, including the use of ground-to-air heat exchanger. This is eco-responsible geothermal ventilation system that aims to ventilate a house or building independently. It consists of sucking in outside air and returning it, after a thermal exchange between the air and the ground, fresh or warm inside a house. Great attention has been paid to this technology in recent years [2]-[13].

A numerical study was carried out by Ramirez-Davila *et al.* [14] to predict the thermal behaviour of a ground-to-air heat exchanger for the extreme heat period in summer and the low temperature period in winter. A numerical fluid mechanics code based on the finite volume method was developed to model the ground-to-air heat exchanger. Simulations were carried out for sand, silt and clay soil textures. The simulation results show that the thermal performance of the ground-to-air heat exchanger is better in summer than in winter, decreasing the air temperature by an average of 6.6˚C and 3.2˚C in summer and increasing it by 2.1˚C and 2.7˚C in winter, respectively. The analysis of the nature of the soil showed that the use of the ground-to-air heat exchanger is appropriate for heating or cooling buildings in extreme and moderate temperature zones where the thermal inertia effect in the soil is higher.

A thermal model of a vaulted roof building integrated with a ground-to-air heat exchanger was studied by Chel *et al.* [15]. The energy balance equations of the building with six interconnected rooms were solved simultaneously using the fourth order Runge-Kutta numerical technique. The results of the thermal model were validated with experimental data. The results show that the annual energy saving potential of the building before and after the integration of the air-to-ground heat exchanger was 4946 kWh/year and 10,321 kWh/year respectively. This significant increase in the building's annual energy savings potential with the air-to-ground heat exchanger resulted in a reduction in CO_2 emissions of

approximately 16 tonnes/year and the corresponding annual carbon credit for the building was estimated at $340/year. The life cycle cost analysis shows that the payback period is less than 2 years for the investment in the ground-to-air heat exchanger system.

The heating potential of a single ground-to-air heat exchanger as well as a system of multiple parallel buried tubes was studied by Mihalakakou *et al.* [16] using real climate data. The dynamic thermal performance of the system during the winter period and its operational limits were calculated in Ireland using a numerical model. This study shows that the main variables influencing the performance of air-to-ground heat exchangers are the length of the tube, the radius of the tube, the air velocity inside the tube and the depth of the tube below the earth's surface.

The work of Vaz *et al.* [17] is devoted to the experimental and numerical study of ground-to-air heat exchangers, which are used to reduce the conventional energy consumption for heating and cooling of buildings by using the thermal energy contained in the ground. The numerical solution of the conservation equations of the problem is performed with a commercial code (FLUENT) which is based on the finite volume method (FVM). The turbulence is treated with the Reynolds stress model (RSM). The numerically predicted transient temperature fields were compared with the experimental fields, the largest difference found being less than 15%. The results showed the validity and efficiency of the computational model employed, allowing its use for future research and development projects on air-to-ground heat exchangers.

The literature review highlighted aspects of the design of ground-to-air heat exchangers in order to produce thermal comfort in the building and reduce energy consumption for heating or cooling of buildings. It has highlighted the physical phenomena involved and the geometrical and physical parameters that influence the thermal behavior of this system. However, few works have been done to examine the influence of the nature of the soil on the passive cooling potential of ground-to-air heat exchangers. Most of the models do not rigorously take into account the dynamics of the air flow in the tubes. Therefore, to our knowledge, there is no database available on the air conditioning potential of ground-to-air heat exchangers in the climatic conditions of Togo. The present work aims to contribute to a better understanding of the heat transfers within the ground-to-air exchanger through a rigorous numerical model taking into account the flow dynamics and the climatic conditions of Togo, which is a warm climate African country. This work also focuses on the influence of the soil type on the distribution of velocities, temperatures, humidity and thermal efficiency of the ground-to-air heat exchanger in order to determine which type of soil would be more suitable for ground-to-air heat exchangers installations.

2. Problem Formulation

2.1. Problem Configuration and Assumptions

The problem to be investigated consists of a buried U-shaped tube with a length

L and a diameter D at a depth H of the surface of the soil through which air flows. The Schematic diagram of the physical model is presented in Figure 1. The ground-to-air heat exchanger is divided into three compartments: the left vertical column (Compartment 1), the horizontal tube (compartment 2) and the right vertical column (compartment 3). In this investigation, two-dimensional unsteady flow characteristics are assumed. The assumptions of the Boussinesq approximation are utilized while modeling the energy equation. The fluid is Newtonian and incompressible. The flow regime is considered to be laminar. It is neglected heat transfer by radiation. The viscous dissipation and the pressure term in the heat equation are negligible.

2.2. Governing Equations

The governing system of equations representing the conservation equations for mass, momentum, energy and vapour concentration [18] [19] under the given assumptions in the dimensionless model are given as:

Continuity equation:

$$\frac{\partial U}{\partial X}+\frac{\partial V}{\partial Y}=0 \tag{1}$$

Momentum equation:

-following x axis:

$$\frac{\partial U}{\partial \tau}+U\frac{\partial U}{\partial X}+V\frac{\partial U}{\partial Y}=-\frac{\partial P}{\partial X}+\frac{1}{R_e}\left(\frac{\partial^2 U}{\partial X^2}+\frac{\partial^2 U}{\partial Y^2}\right) \tag{2}$$

-following y axis:

$$\frac{\partial V}{\partial \tau}+U\frac{\partial V}{\partial X}+V\frac{\partial V}{\partial Y}=-\frac{\partial P}{\partial X}+\frac{1}{R_e}\left(\frac{\partial^2 V}{\partial X^2}+\frac{\partial^2 V}{\partial Y^2}\right)+R_{iT}\theta+R_{iM}C \tag{3}$$

Energy equation:

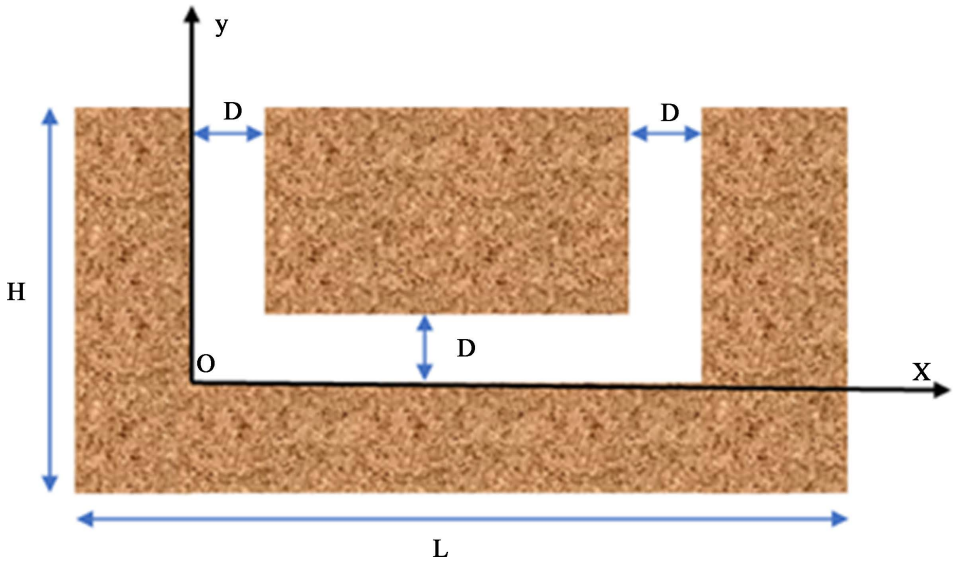

Figure 1. Schematic diagram of ground-to-air heat exchanger.

$$\frac{\partial\theta}{\partial\tau}+U\frac{\partial\theta}{\partial X}+V\frac{\partial\theta}{\partial Y}=\frac{1}{RePr}\left(\frac{\partial^2\theta}{\partial X^2}+\frac{\partial^2\theta}{\partial Y^2}\right) \tag{4}$$

Vapour concentration equation:

$$\frac{\partial C}{\partial\tau}+U\frac{\partial C}{\partial X}+V\frac{\partial C}{\partial Y}=\frac{1}{ScRe}\left(\frac{\partial^2 C}{\partial X^2}+\frac{\partial^2 C}{\partial Y^2}\right) \tag{5}$$

where $Ri=\frac{Gr}{Re^2}$ and $Ri_M=\frac{Gr_M}{Re^2}$ are respectively thermal and mass Richardson numbers;

$Gr=\frac{g\cdot\beta\cdot\Delta T\cdot L^3}{\nu^2}$ and $Gr_M=\frac{g\cdot\beta\cdot\Delta C\cdot L^3}{\nu^2}$ are respectively thermal and mass Grashof number;

$Re=\frac{UL}{\nu}$ is Reynolds number; $Pr=\frac{\upsilon}{\alpha}$ is Prandtl number; $Sc=\frac{\mu}{\rho D}$ is Schimidt number.

The employed dimensionless variables used in the governing equations are:

$$X=\frac{x}{H};\ Y=\frac{y}{H};\ U=\frac{u}{V_0};\ V=\frac{v}{V_0};\ \tau=t\frac{V_0}{H};\ C=\frac{c-c_e}{c_{tube}-c_e}; \tag{6}$$

$$\theta=\frac{T-\bar{T}_{soil}}{\bar{T}_e-\bar{T}_{soil}};\ \theta_{soil}=\frac{T_{sol}-\bar{T}_{sol}}{\bar{T}_e-\bar{T}_{sol}};\ \theta_{amb}=\frac{T_{amb}-\bar{T}_{soil}}{\bar{T}_e-\bar{T}_{soil}} \tag{7}$$

With V_0, $\bar{T}_e$, c_e are inlet values of velocity, temperature and vapour concentration. $\bar{T}_{soil}$ is the soil average temperature.

2.3. Boundary Conditions

The proposed problem is subjected to the following boundary conditions in the dimensionless form:

- at the inlet of earth-air heat exchanger: $0\le X\le\frac{D}{H}$, $Y=1$

$$U=0;\ V=-1;\ \theta=\theta_{amb};\ C=0 \tag{8}$$

- at the outlet of earth-air heat exchanger: $\frac{L-D}{H}\le X\le\frac{L}{H}$, $Y=1$

$$\left.\frac{\partial U}{\partial Y}\right|_{Y=1}=0;\ \left.\frac{\partial V}{\partial Y}\right|_{Y=1}=0;\ \left.\frac{\partial\theta}{\partial Y}\right|_{Y=1}=0;\ \left.\frac{\partial C}{\partial Y}\right|_{Y=1}=0; \tag{9}$$

- on the left vertical wall of compartment 1: $X=0$; $0\le Y\le 1$

$$U=U=0;\ \theta=\theta_{sol};\ C=1 \tag{10}$$

- on the right vertical wall of compartment 1: $X=\frac{D}{H}$; $\frac{D}{H}\le Y\le 1$

$$U=U=0;\ \theta=\theta_{sol};\ C=1 \tag{11}$$

- on the lower horizontal wall of compartment 2: $0\le X\le\frac{L}{H}$, $Y=0$

$$U=U=0;\ \theta=\theta_{sol};\ C=1 \tag{12}$$

- on upper horizontal wall of compartment 2: $\frac{D}{H} \le X \le \frac{L-D}{H}$, $Y = \frac{D}{H}$

$$U = V = 0;\ \theta = \theta_{sol};\ C = 1 \tag{13}$$

- on the left vertical wall of compartment 3: $X = \frac{L-D}{H}$; $\frac{D}{H} \le Y \le 1$

$$U = U = 0;\ \theta = \theta_{sol};\ C = 1 \tag{14}$$

- on the right vertical wall of compartment 3: $X = \frac{L}{H}$; $0 \le Y \le 1$

$$U = U = 0;\ \theta = \theta_{sol};\ C = 1 \tag{15}$$

2.4. Heat Conservation Equation in the Soil

In the study of the air-soil heat exchanger the soil is considered as a semi-infinite medium. In this condition, the heat equation of the soil can be written as:

$$\frac{\partial T_{sol}}{\partial t} = \alpha_{sol} \frac{\partial^2 T_{sol}}{\partial z^2} \tag{16}$$

The boundary conditions are as follow:

$$T_{sol}(0,t) = T_0 + A_T \cos\left[\omega\left(t - t_0\right)\right] \tag{17}$$

$$T_{sol}(\infty,t) = T_0 \tag{18}$$

$$\text{With: } T_0 = \frac{T_{\min} + T_{\max}}{2} \text{ and } A_T = \frac{T_{\max} - T_{\min}}{2} \tag{19}$$

The analytical solution of this equation is given as (24):

$$T_{Sol}(z,t) = T_0 + A_T \exp\left(-z\sqrt{\frac{\omega}{2\alpha_{sol}}}\right) \cdot \cos\left(\omega\left(t - t_0\right) - z\sqrt{\frac{\omega}{2\alpha_{sol}}}\right) \tag{20}$$

With:

$$Z = H - y \tag{21}$$

2.5. Heat Transfer Rate

The rate of heat transfer between the air and the walls of the ground-to-air heat exchanger heat transfer is characterized by the local Nusselt number (Nu) and average Nusselt number ($\bar{N}u$) estimated respectively as:

$$Nu = \left.\frac{\partial\theta}{\partial Y}\right|_{Y=0} + \left.\frac{\partial\theta}{\partial Y}\right|_{Y=D/H} + \left.\frac{\partial\theta}{\partial X}\right|_{X=0} + \left.\frac{\partial\theta}{\partial X}\right|_{X=D/H} + \left.\frac{\partial\theta}{\partial X}\right|_{X=(L-D)/H} + \left.\frac{\partial\theta}{\partial X}\right|_{X=L/H} \tag{22}$$

$$\begin{aligned}\bar{N}u = {} & \frac{H}{L}\int_0^{L/H} \left.\frac{\partial\theta}{\partial Y}\right|_{Y=0} \mathrm{d}X + \frac{H}{L-2D}\int_{D/H}^{(L-D)/H} \left.\frac{\partial\theta}{\partial Y}\right|_{Y=D/H} \mathrm{d}X \\ & + \int_0^1 \left.\frac{\partial\theta}{\partial X}\right|_{X=0} \mathrm{d}Y + \frac{H}{H-D}\int_{D/H}^1 \left.\frac{\partial\theta}{\partial X}\right|_{X=D/H} \mathrm{d}Y \\ & + \frac{H}{H-D}\int_{D/H}^1 \left.\frac{\partial\theta}{\partial X}\right|_{X=(L-D)/H} \mathrm{d}Y + \int_0^1 \left.\frac{\partial\theta}{\partial X}\right|_{X=L/H} \mathrm{d}Y\end{aligned} \tag{23}$$

2.6. Efficiency of Ground-to-Air Heat Exchanger

The efficiency of the ground-to-air heat exchanger is evaluated as:

$$Eff = \frac{\overline{T}_{out} - \overline{T}_{in}}{\overline{T}_{soil} - \overline{T}_{in}} \tag{24}$$

with:

T_{out} : The average temperature at the outlet of the exchanger;

T_{in} : Average temperature at the inlet of the exchanger;

$\overline{T}_{soil}$: Average temperature of the soil at the exchanger's burial depth.

3. Numerical Method and Validation

3.1. Numerical Method

The finite difference method with Alternating Direction Implicit (ADI) scheme is used to discretize the governing equations. The system of algebraic equations is solved iteratively by means of the Thomas algorithm. In order to stop this iterative process, the following stopping criteria are prescribed:

$$\left| \frac{\Gamma^{n+1} - \Gamma^{n}}{\Gamma^{n+1}} \right| \leq 10^{-6} \tag{25}$$

where Γ represents a dependent variable U, V, θ and C. Here, the iteration counter is denoted by superscript n. The convergence of the iterative process is ensured using a sub-relaxation coefficient of 0.8.

3.2. Grid Independency

In order to determine a proper grid for the numerical simulation, a grid independence study is under taken for mixed convection in ground-to-air heat exchanger tube for D = 0.4 m, L = 5 m, H = 1 m, Ra = 105, Ri = 10 and Pr = 0.72. With six different uniform grids, namely: 151 × 101, 171 × 121, 191 × 141, 201 × 181, 211 × 191 and 221 × 201 employed and for each grid size, stream function and temperature values are obtained at the point (x = 2.0 m, y = 0.7 m) aas shown in Table 1. Reasonably good agreement was found between the grids 201 × 181 and 211 × 191. Therefore, to further study, the grid 201 × 181 with lower cells was considered.

Table 1. Accuracy test for D = 0.4 m, L = 5 m, H = 1 m, Ra = 105, Ri = 10 and Pr = 0.72.

Nodes	φ (0.2, 0.7)	T (0.2, 0.7)
151 × 101	−0.00321	303.049
171 × 121	−0.00412	303.043
191 × 141	−0.00108	303.055
201 × 181	−0.00115	303.056
211 × 191	−0.00116	303.057
221 × 201	−0.00149	303.044

3.3. Validation

The present numerical scheme was validated against the numerical results obtained by Aydin *et al.* [20]. **Figure 2** shows the comparison of streamlines and isotherms between the present numerical results and that of Aydin *et al.* [20]. As can be seen, there is excellent agreement between the present work and the results

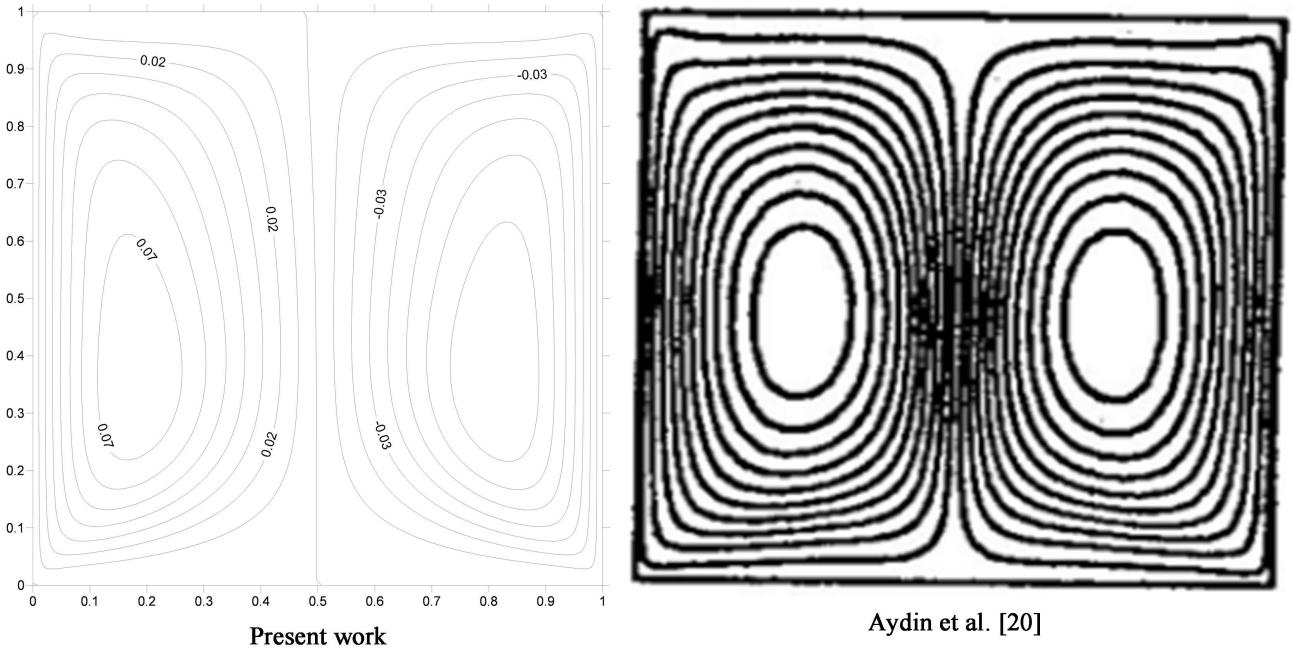

Figure 2. Comparison of streamlines and isotherms between the present numerical results and that of Aydin *et al.* [20] for $\varepsilon = \frac{1}{5}$, $Re = 100$ and $Ri = 10$.

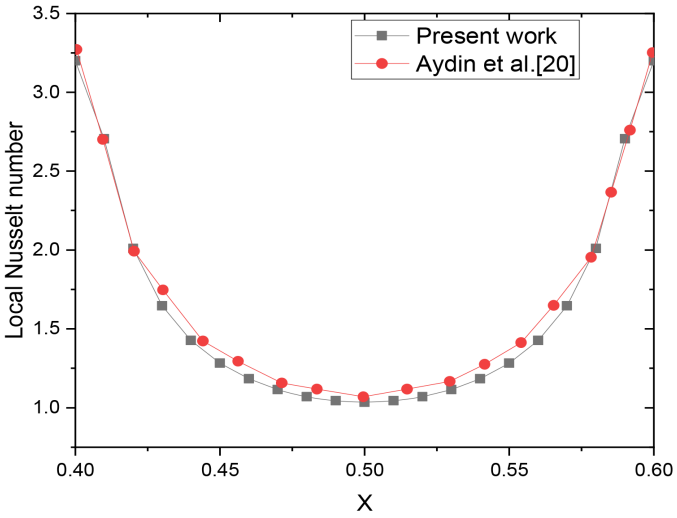

Figure 3. Comparison of streamlines and isotherms between the present numerical results and that of Aydin *et al.* [20] for $\varepsilon = \frac{1}{5}$, $Re = 100$ and $Ri = 10$.

obtained by Aydin *et al.* [20]. The variation of local Nusselt number at the heated wall versus x coordinate of this work and that of Aydin *et al.* [20] are also compared (**Figure 3**). It is found that the results are well overlapped. The difference in results is less than 5%. Therefore, the local Nusselt number of the present study agrees well with that of Aydin *et al.* [20]. The slight discrepancies between the results would be due to the physical properties of the air and the numerical schemes used.

4. Results and Discussion

The simulation of the operation of the ground-to-air heat exchanger is carried out using climatic data for Togo (**Table 2**) for 2021. We have taken into account in this work the influence of the soil nature by considering three types of dry soil: clay soil, sandy-clay soil and sandy soil whose physical properties are presented in **Table 3** [21]. The results obtained from the investigation of soil nature effect on the passive cooling of rooms using ground-to-air heat exchanger are discussed in this section. The numerical results are presented in terms of contours of streamlines, isotherms and isoconcentration as well as the variation with abscissa x of the vertical and horizontal velocity components, temperature, concentration at selected depths below the soil surface. The evolution of average Nusselt number at the walls and effectiveness of the geothermal system are also highlighted. To better present the results, the domain studied is divided into three compartments: Compartment 1 for the left vertical column of the tube, compartment 2 for the right vertical column and compartment 3 for the horizontal part of the tube.

4.1. Flow Fields

Figure 4 shows the distribution of the streamlines according to the nature of the

Table 2. Climate data of Togo (National meteological Service of National Aviation Security Agency (ASECNA)).

Months	Temperature (˚C)	Solar Flux Density (W·m^{-2})
January	28.5	591.9
February	29.7	714.3
March	29.9	750.0
April	28.7	800.4
May	27.8	705.0
June	26.5	570.8
July	25.4	691.2
August	24.5	584.8
September	25.3	758.6
October	27.1	776.5
November	28.0	690.5
December	28.3	617.0

Table 3. Thermal properties of dry soil [21].

Type of soil	ρ_{soil} (kg/m^3)	a_{soil} (m^2/s)	C_{psoil} (J/kg·˚C)
Clay soil	1500	9.69×10^{-7}	880
Sandy-clay silt soil	1800	6.22×10^{-7}	1340
Sandy soil	1780	3.76×10^{-7}	1390

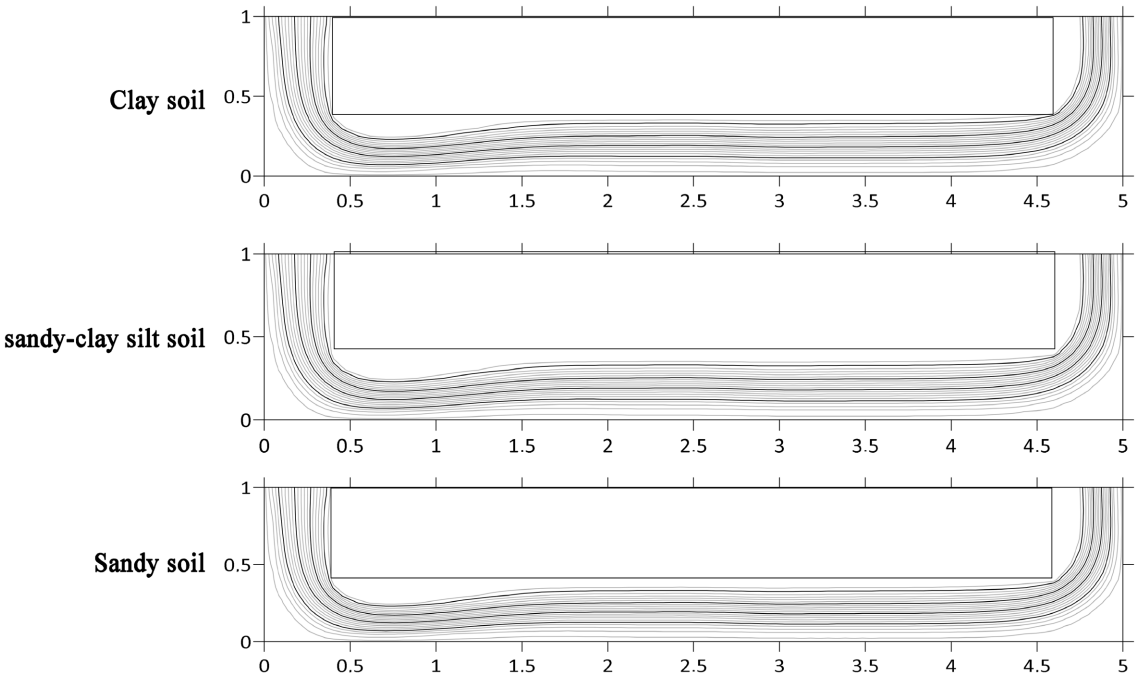

Figure 4. Distribution of streamlines under the influence of soil type; $L = 5$ m; $D = 4$ m; $H = 1$ m; Re = 400.

soil. For the three kinds of soils considered, the flow structure is composed of open streamlines denoting the domination of forced convection. It can be seen that the distribution of the streamlines is not significantly affected by the nature of the soil in which the tube of ground-to-air heat exchanger has been buried. This result is corroborated by the variation of the flow velocity components as a function of the abscissa for different categories of soil characterized by their diffusivities (Figure 5 and Figure 6). No change is observed for sandy soil, clay soil and sandy-clay silt soil.

4.2. Temperature Fields

The distribution of isotherms under the influence of soil type is shown in Figure 7. The analysis of this figure shows that the isotherms are very little modified by the variation of the soil type. Small changes are observed at the horizontal part of the exchanger near the right-hand bend. In different cases, the contours of isotherm have a lanceolate shape with the tip pointing in the direction of flow and are parallel to the walls, indicating heat transfer by convection-conduction between the walls and the air. The temperature profiles for the different soil types presented in Figure 8 corroborate with the description of the isotherms made earlier. There is a slight variation in the profiles in compartment 1 which is dominated by a high air flow velocity. However, strong variations are observed in compartments 2 and 3 of the ground-to-air heat exchanger. The temperature values obtained for the clay soil are higher while the sandy soil shows lower temperature values. The temperatures of the sandy clay soil are intermediate between those of the clay and sandy soils. This result shows that a sandy soil would be more suitable for geothermal system installations.

4.3. Heat Transfer Rate

Figure 9 presents the temporal variation of the average Nusselt number under the influence of the soil properties. It can be seen that, for different types of soil considered, the average Nusselt number decreases with time. This indicates a decrease in heat transfer over time due to the very small temperature gradient between the walls of the exchanger and the air. The evolution of the average Nusselt number (Figure 9) characterizing the intensity of heat transfer indicates that the values of the average Nusselt number are higher for a sandy soil than for a sandy-clay soil. The lowest values of the Nusselt number are observed for a clay soil. The heat transfer is therefore more intense for sandy soil and less intense for clay soil.

4.4. Humidity Fields

Figure 10 and Figure 11 show, respectively, the distribution of moisture isolines and the moisture profiles in different sections of the exchanger for different soil types (clay soil, sandy-clay silt soil and clay soil). Examination of these figures reveals that the nature of the soil, via thermal diffusivity, does not significantly

influence the spatial distribution of moisture in the exchanger. The natural convection generated by the temperature gradients between the air and the walls of the exchanger is not sufficient to significantly modify the spatial distribution of

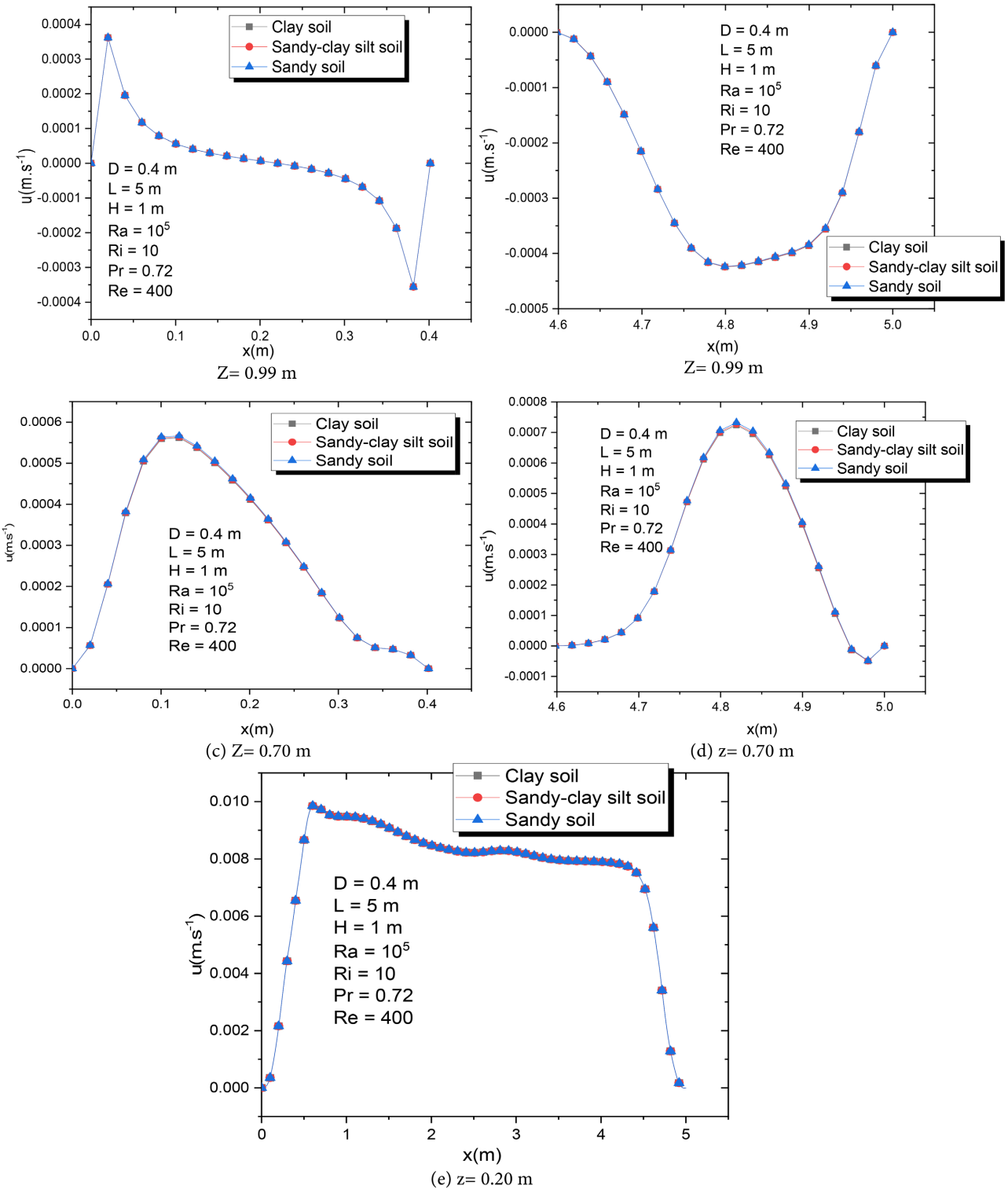

Figure 5. Profiles of the u component of the velocity as a function of the abscissa *x* in the air/soil exchanger under the influence of the soil type.

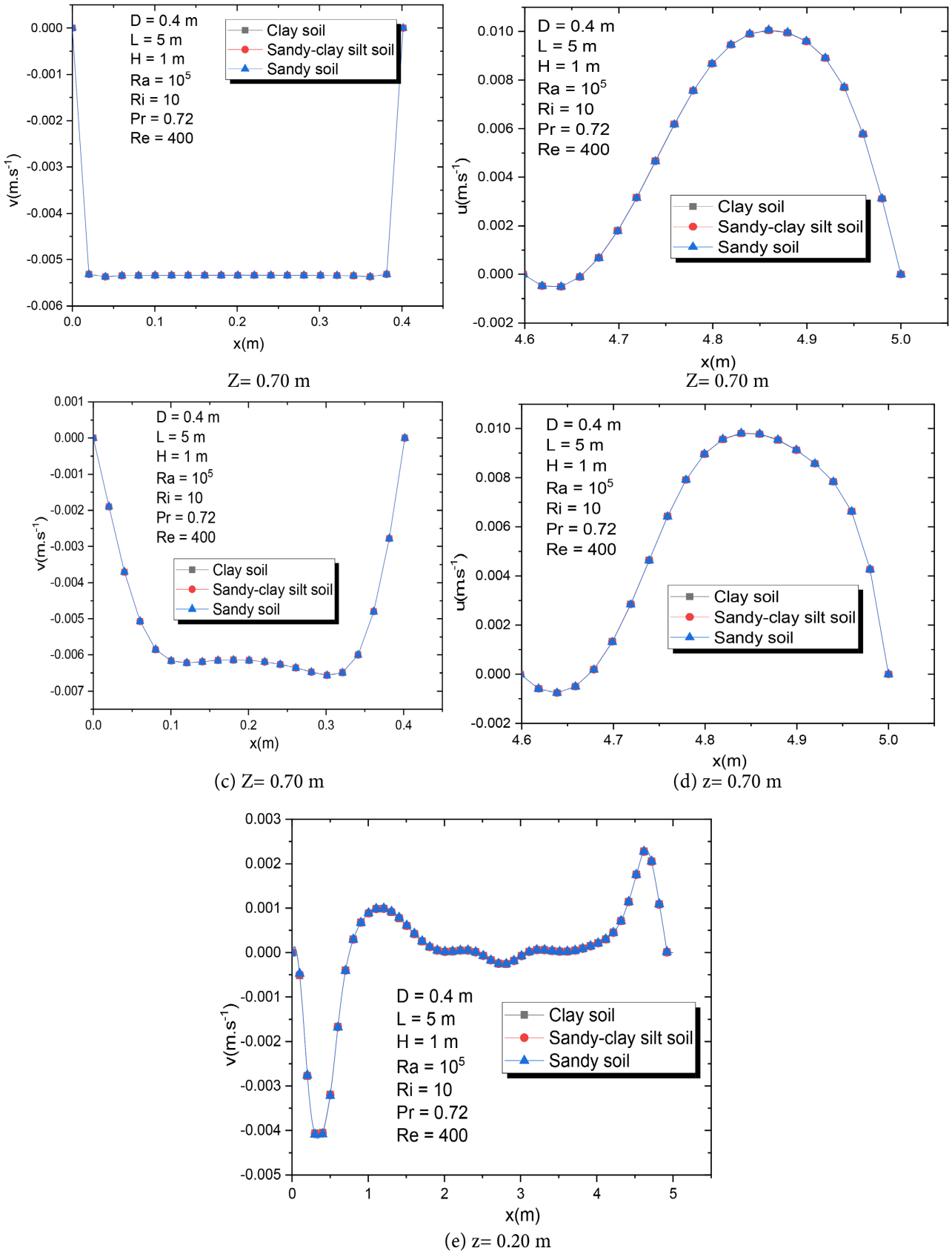

Figure 6. Profiles of the velocity component v as a function of x in the air/soil exchanger under the influence of the soil type.

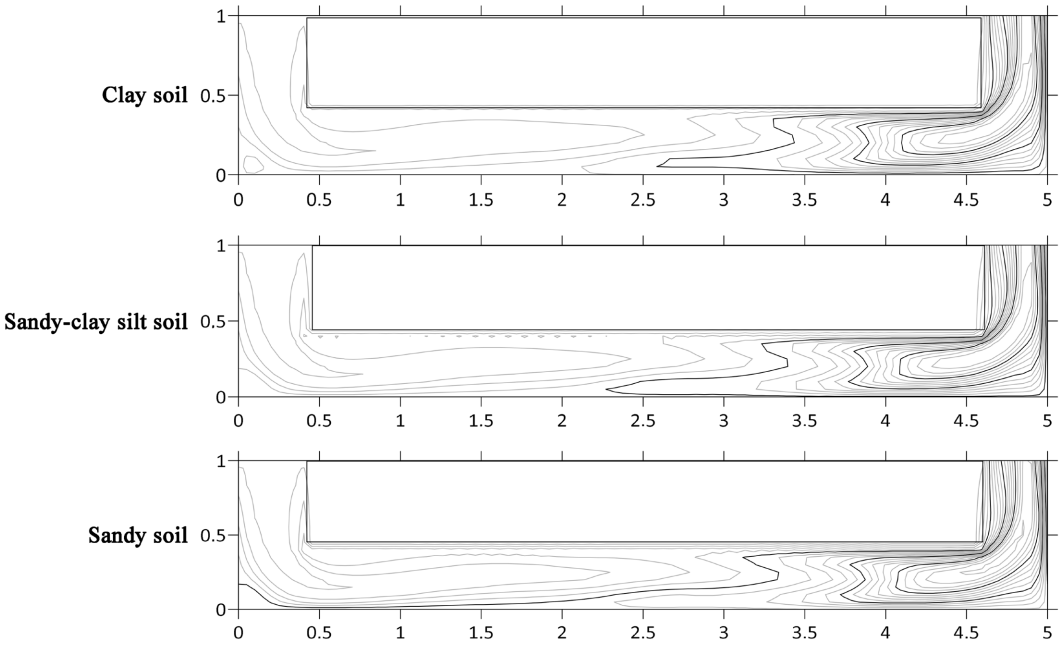

Figure 7. Distribution of isotherms under the influence of soil type; $L = 5$ m; $D = 4$; $H = 1$ m; $Re = 400$.

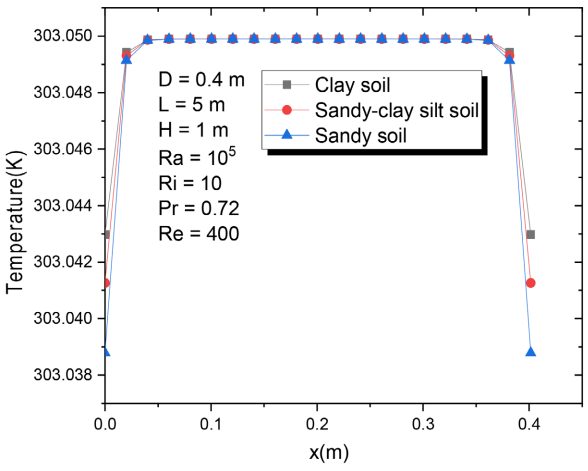

Z= 0.99 m

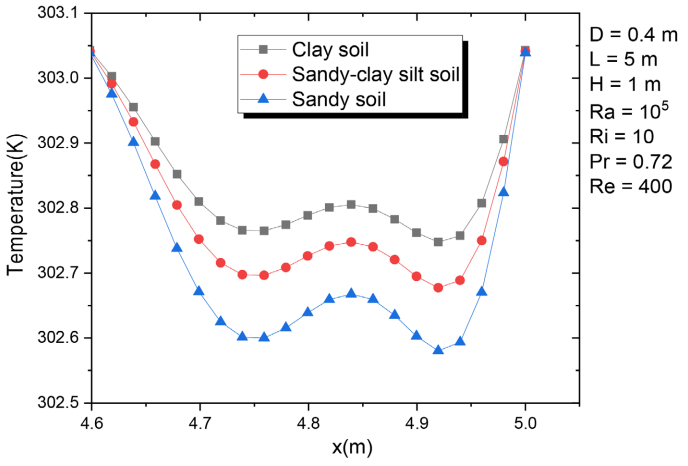

Z= 0.99 m

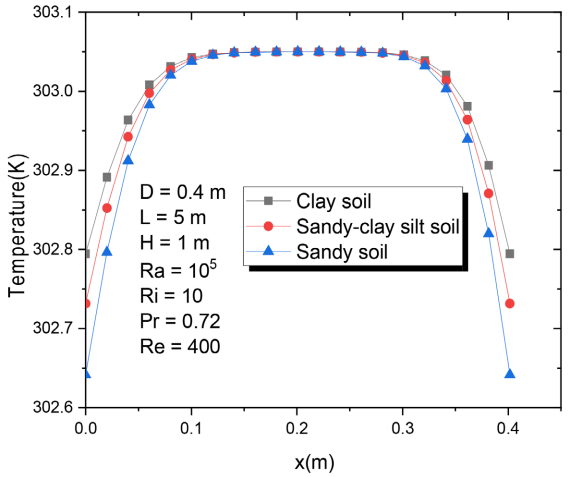

(c) Z= 0.70 m

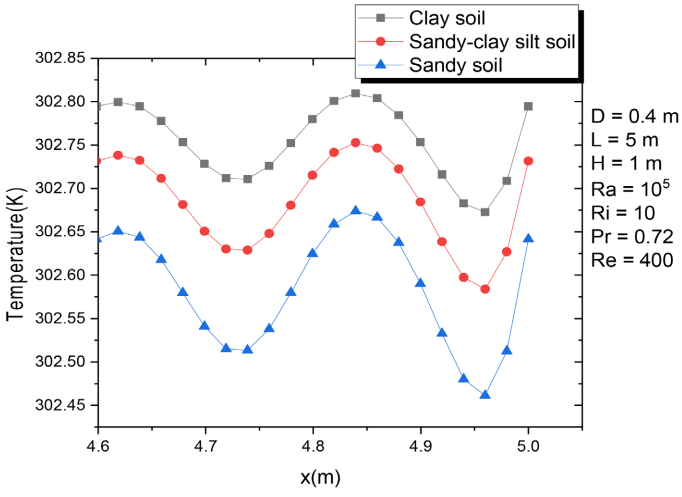

(d) z= 0.70 m

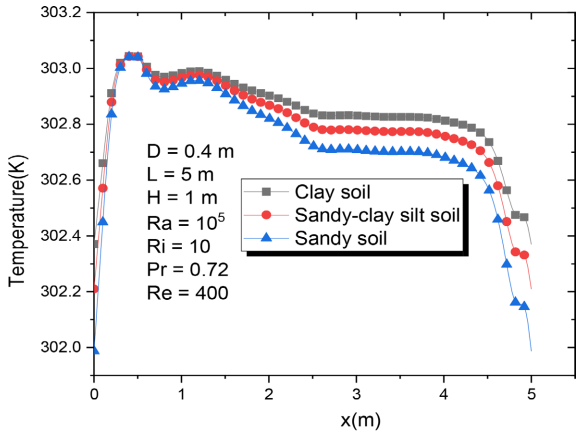

(e) z= 0.20 m

Figure 8. Temperature profiles as a function of x in the air/soil exchanger under the influence of the soil type.

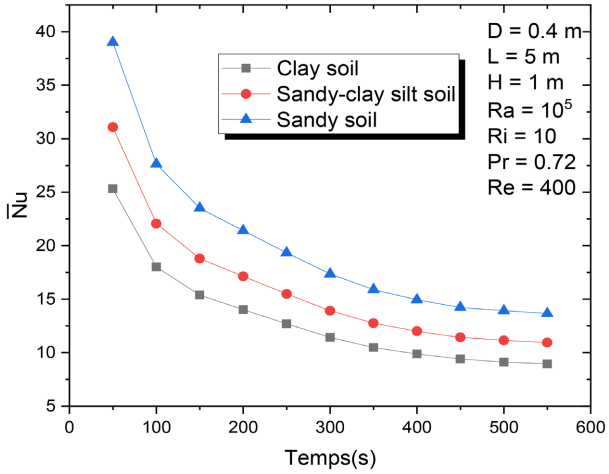

Figure 9. Evolution of the average Nusselt number under the influence of the soil type.

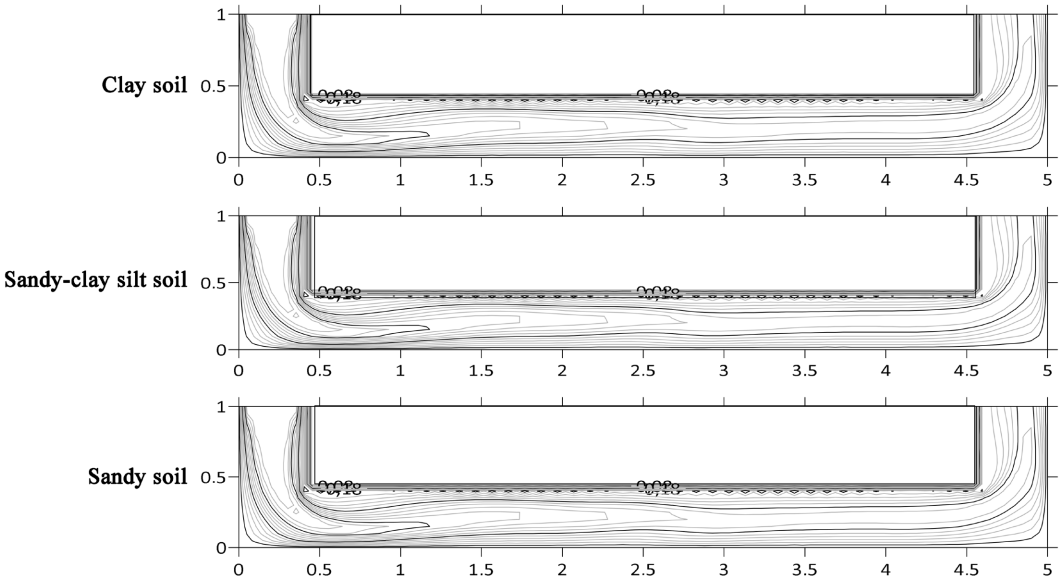

Figure 10. Distribution of moisture isovals under the influence of soil type; $L = 5$ m; $D = 4$ m; $H = 1$ m; $Re = 400$.

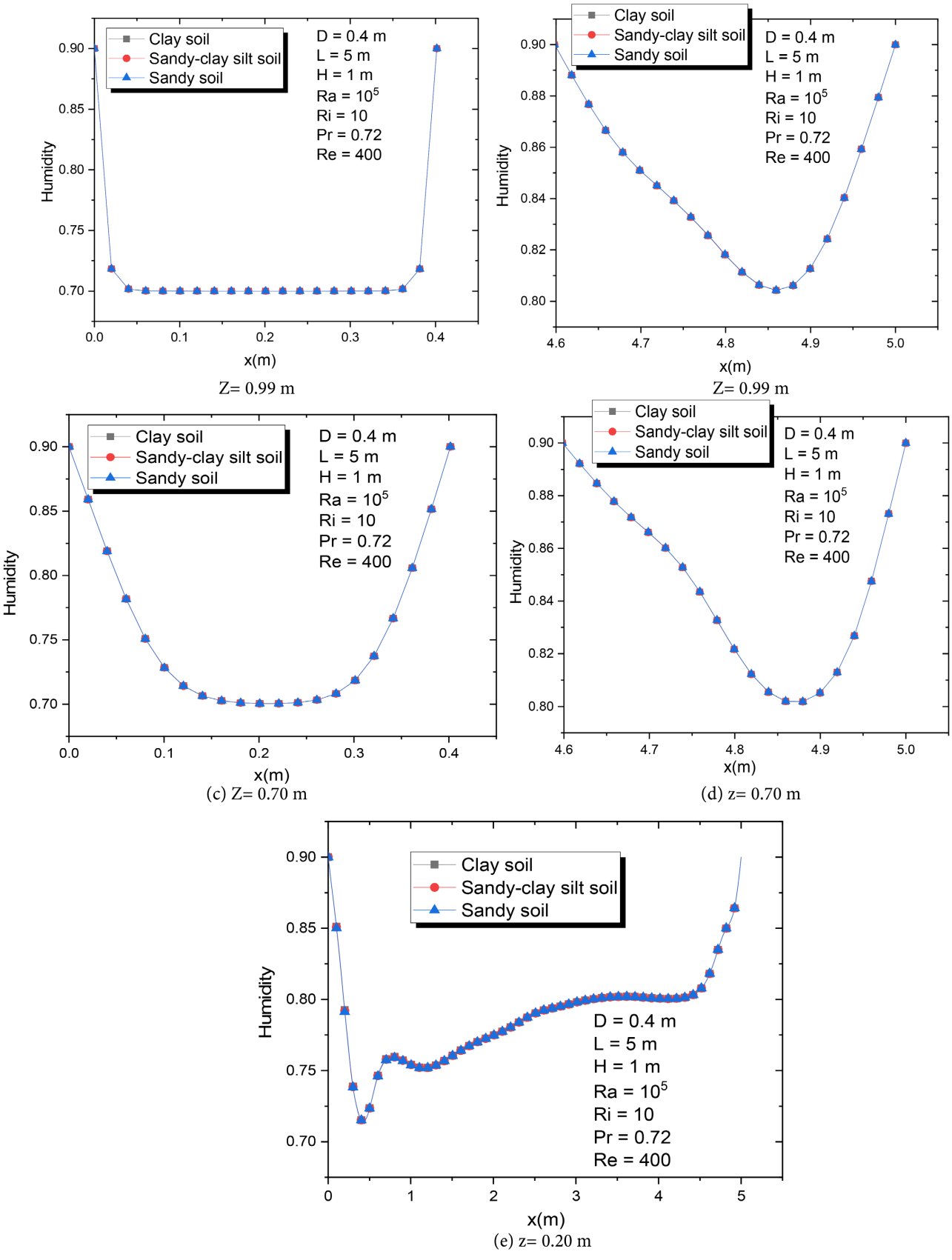

Figure 11. Moisture profiles as a function of x in the air/soil exchanger under the influence of the soil type.

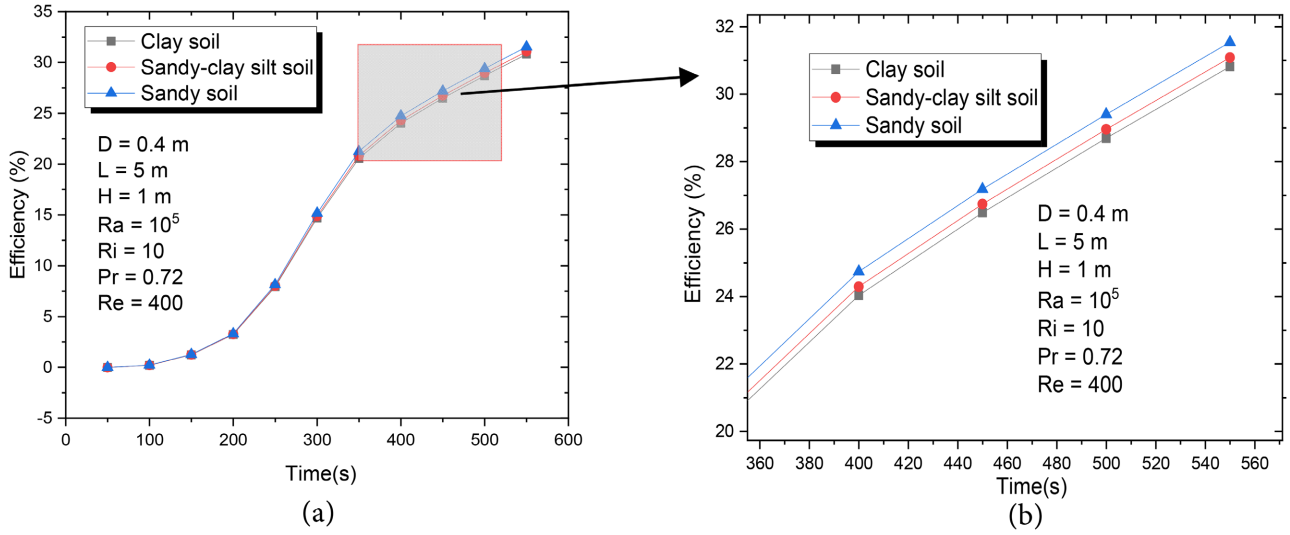

Figure 12. Evolution of the efficiency of the earth-air heat exchanger under the influence of the soil type.

the moisture. This is due to the fact that the thermal diffusivities of different types of soil are of the same order of magnitude. The distribution of humidity isovalues is similar to that of temperature. In the vicinity of the walls these lines are very tight and parallel to the walls. This distribution shows that moisture transfer is more intense in these areas.

4.5. Earth-Air Heat Exchanger Efficiency

The investigation of the influence of the nature of the soil on the evolution of the ground-to-air heat exchanger efficiency is presented in **Figure 12**. The analysis of this figure shows that the efficiency of the air/soil exchanger increases with time. It can be seen in this figure that the values of the ground-to-air heat exchanger efficiency are only slightly influenced by the nature of the soil. Nevertheless, we note a slightly better efficiency for the sandy soil than for the sandy-clayey silt and clayey soils.

5. Conclusions

In the present work, heat transfer within the ground-to-air heat exchanger is studied taking into account three types of soil namely: clay soil, sandy soil, sandy-clay silt soil. The analysis is performed numerically using finite difference method. The investigation of the effect of the type of the soil on the flow structure, temperature distribution and moisture distribution as well as the average Nusselt number and the efficiency of ground-to-air heat exchanger conducted to the following main results:

- the distributions of contours of streamlines, isotherms, isovalues of moisture are less affected by the type of soil;
- the temperature values obtained for the clay soil are higher while the sandy soil shows lower temperature values;
- the values of the average Nusselt number are higher for a sandy soil than for

a sandy-clay soil; the lowest values of the Nusselt number are observed for a clay soil. The heat transfer is therefore more intense for sandy soil and less intense for clay soil;

- it is noted a slightly better efficiency for the sandy soil than for the sandy-clayey silt and for clayey soils, a sandy soil is more suitable for geothermal system installations than clay soil and sandy-clayey silt soil.

Acknowledgements

The authors thank the Director and staff members of National Metrological Ser-vice of National Aviation Security Agency (ASECNA) of Togo for providing climate data required for this work. They are also grateful to the anonymous reviewers for their thorough reviews, helpful comments and suggestions.

Conflicts of Interest

The authors declare no conflicts of interest regarding the publication of this paper.

References

[1] Pérez-Lombard, L., Ortiz, J. and Pout, C. (2008) A Review on Buildings Energy Consumption Information. *Energy and Buildings*, **40**, 394-398. https://doi.org/10.1016/j.enbuild.2007.03.007

[2] Mihalakakou, G., Souliotis, M., Papadaki, M., Halkos, G., Paravantis, J., Makridis, S. and Papaefthimiou, S. (2022) Applications of Earth-to-Air Heat Exchangers: A Holistic Review. *Renewable and Sustainable Energy Reviews*, **155**, Article ID: 111921. https://doi.org/10.1016/j.rser.2021.111921

[3] Sawhney, R., Buddhi, D. and Thanu, N. (1999) An Experimental Study of Summer Performance of a Recirculation Type Underground Air Pipe Air Conditioning System. *Building and Environment*, **34**, 189-196. https://doi.org/10.1016/S0360-1323(98)00009-2

[4] Santamouris, M., Pavlou, K., Synnefa, A., Niachou, K. and Kolokotsa, D. (2007) Recent Progress on Passive Cooling Techniques Advanced Technological Developments to Improve Survivability Levels in Low-Income Households. *Energy and Buildings*, **39**, 859-866. https://doi.org/10.1016/j.enbuild.2007.02.008

[5] Santamouris, M. and Kolokots, D. (2013) Passive Cooling Dissipation Techniques for Buildings and Other Structures: The State of the Art. *Energy and Buildings*, **57**, 74-94. https://doi.org/10.1016/j.enbuild.2012.11.002

[6] Astina, I.M. and Nugraha, M.Y. (2021) Numerical Simulation of Earth-Air Heat Exchanger Application for Indonesian Simple House Air Conditioning System. *Case Studies in Thermal Engineering*, **28**, Article ID: 101371. https://doi.org/10.1016/j.csite.2021.101371

[7] Jayashankar, B.C., Sawhney, R.L. and Sodha, M.S. (1989) Effect of Different Surface Treatments of the Surrounding Earth on Thermal Performance of Earth-Integrated Buildings. *International Journal of Energy Research*, **13**, 605-619. https://doi.org/10.1002/er.4440130512

[8] Givoni, B. and Katz, L. (1985) Earth Temperatures and Underground Buildings. *Energy and Buildings*, **8**, 15-25. https://doi.org/10.1016/0378-7788(85)90011-8

[9] Omer, A.M. (2008) Ground-Source Heat Pumps Systems and Applications. *Renewable and Sustainable Energy Reviews*, **12**, 344-371. https://doi.org/10.1016/j.rser.2006.10.003

[10] Esen, H., Inalli, M. and Esen, M. (2007) Numerical and Experimental Analysis of a Horizontal Ground-Coupled Heat Pump System. *Building and Environment*, **42**, 1126-1134. https://doi.org/10.1016/j.buildenv.2005.11.027

[11] Singh, R., Sawhneyd, R.L., Lazarus, I.J. and Kishorec, V.V.N. (2018) Recent Advancements in Earth Air Tunnel Heat Exchanger (EATHE) System for Indoor Thermal Comfort Application: A Review. *Renewable and Sustainable Energy Reviews*, **82**, 2162-2185. https://doi.org/10.1016/j.rser.2017.08.058

[12] Bisoniya, T.S., Kumar, A. and Baredar, P. (2013) Experimental and Analytical Studies of Earth-Air Heat Exchanger (EAHE) Systems in India: A Review. *Renewable and Sustainable Energy Reviews*, **19**, 238-246. https://doi.org/10.1016/j.rser.2012.11.023

[13] Lia, H., Ni, L., Liu, G. and Yao, Y. (2019) Performance Evaluation of Earth to Air Heat Exchange (EAHE) Used for Indoor Ventilation during Winter in Severe Cold Regions. *Applied Thermal Engineering*, **160**, Article ID: 114111. https://doi.org/10.1016/j.applthermaleng.2019.114111

[14] Ramirez-Davila, L., Xaman, J., Arce, J., Álvarez, G. and Hernandez-Perez, I. (2014) Numerical Study of Earth-to-Air Heat Exchanger for Three Different Climates. *Energy and Buildings*, **6**, 238-248. https://doi.org/10.1016/j.enbuild.2014.02.073

[15] Chel, A. and Tiwari, G.N. (2009) Performance Evaluation and Life Cycle Cost Analysis of Earth to Air Heat Exchanger Integrated with Adobe Building for New Delhi Composite Climate. *Energy and Buildings*, **41**, 56-66. https://doi.org/10.1016/j.enbuild.2008.07.006

[16] Mihalakakou, G., Santamouris, M. and Asimakopoulos, D. (1994) Modelling the Thermal Performance of Earth-to-Air Heat Exchangers. *Soil Energy*, **53**, 301-305. https://doi.org/10.1016/0038-092X(94)90636-X

[17] Vaz, J., Sattler, M.A., dos Santos, E.D. and Isoldi, L.A. (2011) Experimental and Numerical Analysis of an Earth-Air Heat Exchanger. *Energy and Buildings*, **43**, 2476-2482. https://doi.org/10.1016/j.enbuild.2011.06.003

[18] Landau, L.D. and Lifshitz, E.M. (1987) Fluid Mechanics. 2nd Edition, Butterworth-Heinemann, Oxford.

[19] Granger, R.A. (1995) Fluid Mechanics. Dover Publications, Inc., New York.

[20] Aydin, O. and Yang, W.J. (2000) Mixed Convection in Cavities with a Locally Heated Lower Wall and Moving Sidewalls. *Numerical Heat Transfer, Part A: Applications: An International Journal of Computation and Methodology*, **37**, 695-710. https://doi.org/10.1080/104077800274037

[21] Benhammou, M. and Draoui, B. (2011) The Modeling of Soil Temperature in Depth for the Region of Adrar—Effect of the Nature of Soil. *Revue des Energies Renouvelables*, **14**, 219-228.

Nomenclature

Symbol Description

c	dimensionless moisture
C	dimensional moisture (%)
C_{in}	inlet moisture (%)
$\overline{c}_{tube}$	internal face of the tube average moisture
D	diameter of the buried tube (m)
E	earth-air heat exchanger efficiency (%)
Gr_T	thermal Grashof number ($Gr_T = \frac{g \cdot \beta_T \cdot \Delta T \cdot L^3}{\nu^2}$)
Gr_M	mass Grashof number ($Gr_M = \frac{g \cdot \beta_M \cdot \Delta C \cdot L^3}{\nu^2}$)
H	depth of the earth-to-air heat exchanger
L	length of horizontal part of buried tube
Nu	local Nusselt number
$\overline{Nu}$	average Nusselt number
Pr	Prandtl number ($Pr = \nu/\alpha$)
Re	Reynolds number ($Re = \frac{V_{in} L}{\nu}$)
Ri_T	thermal Richardson number ($Ri_T = \frac{Gr_T}{Re^2}$)
Ri_M	mass Richardson number ($Ri_M = \frac{Gr_M}{Re^2}$)
Sc	Schmidt number ($Sc = \frac{\mu}{\rho D}$)
t	dimensional (s)
T	dimensional air temperature in the tube (K)
$\overline{T}_{in}$	inlet air average temperature (K)
$T_{\min}$	minimum average temperature of the year (K)
$T_{\max}$	maximum average temperature of the year (K)
T_{out}	average temperature at the outlet of the exchanger (K)
T_{soil}	soil temperature (K)
$\overline{T}_{soil}$	soil average temperature (K)
u	dimensional velocity component in x-direction ($m \cdot s^{-1}$)
U	non-dimensional velocity component in X-direction
v	dimensional velocity component in y-direction ($m \cdot s^{-1}$)
V	non-dimensional velocity component in Y-direction
V_{in}	inlet velocity ($m \cdot s^{-1}$)
x	Cartesian coordinate in horizontal direction (m)
X	non-dimensional coordinate in horizontal direction
y	Cartesian coordinate in vertical direction (m)
Y	non-dimensional coordinate in vertical direction

Greek Symbols

α	air thermal diffusivity ($m^2 \cdot s^{-1}$)
α_{soil}	soil thermal diffusivity ($m^2 \cdot s^{-1}$)
θ	non-dimensional air temperature in the tube
θ_{soil}	non-dimensional soil temperature
τ	dimensionless time
μ	dynamic viscosity ($kg \cdot m^{-1} \cdot s^{-1}$)
ν	cinematic viscosity ($m^2 \cdot s^{-1}$)
ρ	density ($kg \cdot m^{-3}$)

Subscripts

in	inlet
M	mass
min	minimum
max	maximum
out	outlet
soil	relative to the soil
T	thermal
tube	relative to the tube